

Nuclear liquid-gas phase transition studied with antisymmetrized molecular dynamics

Takuya Furuta and Akira Ono

Department of Physics, Tohoku University, Sendai 980-8578, Japan

(Dated: May 10, 2003)

Abstract

Nuclear liquid-gas phase transition is studied by the antisymmetrized molecular dynamics. The time evolution of a many-nucleon system confined in a container is solved for a long time to get a microcanonical ensemble of given energy and volume. The temperature and the pressure are extracted from this ensemble and the caloric curves are constructed. The present work is the first time that a microscopic dynamical model that well describes nuclear multifragmentation reactions is directly applied to get the nuclear caloric curve. The obtained constant pressure caloric curves clearly show the characteristic feature of the liquid-gas phase transition, namely plateau or backbending (negative heat capacity), which is expected for the phase transition in finite systems.

PACS numbers: 24.10.Lx, 02.70.Ns, 24.60.-k, 25.70.Pq

Phase transitions are general interesting phenomena observed or expected in various fields: melting and boiling of condensed matters and atomic clusters [1, 2, 3], decay of hot nuclei [4, 5, 6], transition to quark gluon plasma in high energy nuclear collisions and so on. Phase transition is often defined as the divergence of heat capacity in canonical ensembles. This definition is applicable only to the thermodynamical limit. On the other hand, Gross *et al.* [7, 8, 9] have pointed out that the essence of the phase transition is the anomalous concavity of the entropy $S(E) = \ln \rho(E)$, with $\rho(E)$ being the level density, which can be clearly observed even in finite systems by finding backbending (negative heat capacity) in the microcanonical caloric curves. There have been many attempts to get the microcanonical caloric curves experimentally and theoretically in various fields [2, 3, 10, 11, 12].

In this letter, we will concentrate on the nuclear liquid-gas phase transition that is expected because of the resemblance between the equation of state (EOS) of infinite homogeneous nuclear matter and the Van der Waals EOS. This phase transition is expected to occur at lower density than the normal nuclear density ρ_0 . Such low density is achieved on earth only by nuclear reactions. In nuclear collisions, many fragments are produced as the experimental results. This multifragmentation is considered to be related to the liquid-gas phase transition. Thus a lot of works have been done to get the information about the phase transition from the multifragmentation data [5, 6, 10, 12, 13, 14, 15, 16]. Much effort is still required in order to confirm the existence of the nuclear liquid-gas phase transition by extracting the statistical information from the data that contain nontrivial dynamical effects.

So far, theoretical researches of the nuclear liquid-gas phase transition have been done mainly by considering ideal systems in thermal equilibrium in statistical models [7, 17, 18, 19] that are based on the assumption of equipartition under a given volume (or pressure) and a given energy (or temperature). Some statistical model calculations have already shown the characteristic feature of the phase transition [19]. However, nontrivial dynamical effects in nuclear collisions make it difficult to directly compare the results of statistical models to the multifragmentation data without introducing additional assumptions.

It is therefore desired to have a unified description of the dynamical effects and the statistical effects in nuclear collisions. The microscopic approach with molecular dynamics models [20, 21, 22, 23, 24, 25, 26, 27] is a candidate to satisfy this requirement. In order to discuss what kind of statistical information is contained in the collision results by using

a molecular dynamics model, it is firstly necessary to study ideal systems in equilibrium and make sure that the same model can describe the statistical properties such as phase transition.

The aim of the present work is to demonstrate that the nuclear liquid-gas phase transition can be described by the antisymmetrized molecular dynamics (AMD) that is a microscopic dynamical model based on the degrees of freedom of interacting nucleons. We utilize the same AMD model that has applied to nuclear collisions and successfully reproduced various aspects of experimental data [20, 21, 24, 25, 26]. AMD can also describe the ground state properties of nuclei so that it has been utilized for nuclear structure studies [28]. Therefore one of the advantages of the present study, compared to the statistical model approach, is that the calculation is based on the nucleon-nucleon interaction, rather than the nuclear binding energies and level densities given externally. Another advantage is that the interaction among fragment nuclei and nucleons is taken into account, while it is usually ignored in statistical models by the freeze-out assumption.

There have been several discussions on the question whether the molecular dynamics models can describe the statistical properties of nuclear systems for which quantum and fermionic features are essential [29, 30, 31, 32, 33]. It has been shown that molecular dynamics can be consistent to the quantum and fermionic caloric curve if the wave function is fully antisymmetrized and an appropriate quantum branching process is taken into account [29, 30, 32, 33]. In fact, there are several works [29, 30, 31, 32, 33, 34, 35] that studied nuclear statistical properties of systems in equilibrium, using molecular dynamics models. However, in any of those works, a clear signal of the phase transition, namely plateau or backbending in the caloric curve, has not been obtained if one adopts an appropriate nuclear force that is consistent to the nuclear saturation property. Those works have calculated caloric curves at constant volume or in a harmonic oscillator confining potential, but there have been no attempts to get the caloric curves at constant pressure. Furthermore, most of those molecular dynamics models were specialized for the study of statistical properties, but the same models have not been applied successfully to dynamical collisions. On the other hand, our present study uses the same version of AMD that has already been utilized for nuclear collision simulations [26]. We will also draw the caloric curves at constant pressure which are expected to show the signal of phase transition most clearly.

AMD is a model to calculate the time evolution of many-nucleon systems microscopically

[26]. It uses a fully antisymmetrized product of Gaussian wave packets,

$$\langle \mathbf{r}_1 \dots \mathbf{r}_A | \Phi(Z) \rangle = \det_{ij} \left[\exp \left\{ -\nu \left(\mathbf{r}_j - \frac{\mathbf{Z}_i}{\sqrt{\nu}} \right)^2 \right\} \chi_{\alpha_i}(j) \right]. \quad (1)$$

The complex variables $\{\mathbf{Z}_i; i = 1, \dots, A\}$ represent the centroids of the nucleon wave packets. We take the width parameter $\nu = 0.16 \text{ fm}^{-2}$ and the spin isospin states $\chi_{\alpha_i} = p \uparrow, p \downarrow, n \uparrow,$ and $n \downarrow$. The Gogny force [36] is used as the effective interaction among nucleons. This force is consistent to the saturation property of nuclear matter, and also reproduces the binding energies of ground state nuclei reasonably well [37]. The time development of the system is not only determined by the equation of motion for the wave packet centroids but also by the quantum channel branchings which are incorporated stochastically. As the origins of the quantum branchings, we consider the two-nucleon collisions and the splittings of wave packets. The aim of the latter origin is to respect both the unrestricted single-particle motion in the mean field and the localization of the wave function to form fragments [26], which is also important for the quantum statistical nature [32, 33].

The microcanonical ensemble of given energy and volume is obtained in the following way by using the microscopic time evolution of AMD. The initial state is prepared by putting A nucleons (N neutrons and Z protons) arbitrarily within a fixed radius r_{wall} , and the time evolution of the system is solved by AMD for a long time. In order to confine the system in the container of volume $V = \frac{4}{3}\pi r_{\text{wall}}^3$, we introduce a reflection procedure as described below. The state at each time is regarded as a sample of the statistical ensemble with energy E , volume V and the particle number $A = N + Z$. (The states of the first a few thousand fm/c are discarded in order to remove the dependence on the choice of the initial state.) It should be emphasized that this ensemble is a microcanonical ensemble with a fixed energy E because the initial energy E is conserved through the AMD time evolution.

During the time evolution, in order to keep A nucleons inside the given volume, we reversed the nucleon momentum against the container wall when a nucleon is going out of the container. When a cluster is going out of the container (we regard each two nucleons belong to the same cluster when their distance is less than 2.5 fm), we apply a similar reflection procedure to the center of mass of the cluster. If one applied the reflection procedure to each nucleon in the cluster, the cluster might be spuriously broken by the crash to the wall. This point seems to be ignored in other statistical studies using molecular dynamics [29, 30, 31, 32, 33, 34, 35].

In this letter we consider the $(N, Z) = (18, 18)$ system which is the same system as Refs. [34, 35]. There are several examples indicating that phase transition can exist even in such small systems [1, 2, 3]. The investigations of this system are done for the cases of $r_{\text{wall}} = 4, 5, \dots, 15$ fm, and $E^*/A = 2, 4, \dots, 28$ MeV, where E^* stands for the excitation energy relative to the ground state ^{36}Ar nucleus. The minimum radius $r_{\text{wall}} = 4$ fm corresponds to a volume of the container $V \gtrsim A/\rho_0$, and therefore we do not consider a compressed liquid nucleus in this letter.

The time development was calculated up to 20000 fm/ c , which is much longer than a typical nuclear reaction time scale (~ 100 fm/ c). The states for the first 5000 fm/ c were discarded in order to remove the initial state dependence. Samplings were done at every 10 fm/ c . Similar calculations were carried out 6 times independently to improve the statistics.

The temperature and the pressure are evaluated for each ensemble of given $\{E, V, A\}$ as follows. The microcanonical temperature is defined by $T^{-1} = (\partial S/\partial E)|_{V,A}$. This is evaluated with a good precision by using the average kinetic energy of isolated nucleons which do not have other nucleons in the distance of 2.5 fm. The temperature for the ensemble is obtained by

$$\frac{3}{2}T = \left\langle \frac{K_{\text{iso}}}{N_{\text{iso}}} \right\rangle_{\{E,V,A\}}, \quad (2)$$

where N_{iso} and K_{iso} are the number and total kinetic energy of the isolated nucleons, respectively, for each sample state. The brackets $\langle \rangle_{\{E,V,A\}}$ denote the average value for the microcanonical ensemble with $\{E, V, A\}$. It can be proved analytically that this definition of the temperature coincides with the microcanonical definition of the temperature if the isolated nucleons follow the Maxwell distribution, which is very likely. The pressure is calculated by using the reflection history at the container wall, that is, summing up the magnitudes of the momentum change by the reflection and dividing the sum by the total time and the surface area of the container.

After these calculations, we eventually know the temperature and pressure at each lattice point in the E - V plain. Figure 1a shows the constant volume caloric curves. If the volume is not very small, the temperature smoothly grows in the low energy part up to some point from which the temperature linearly increases with the energy. This result is consistent to the other calculation of Ref. [35] with another version of AMD. For the comparison, in Fig. 1b, we show the caloric curves for the infinite nuclear matter (without Coulomb interaction)

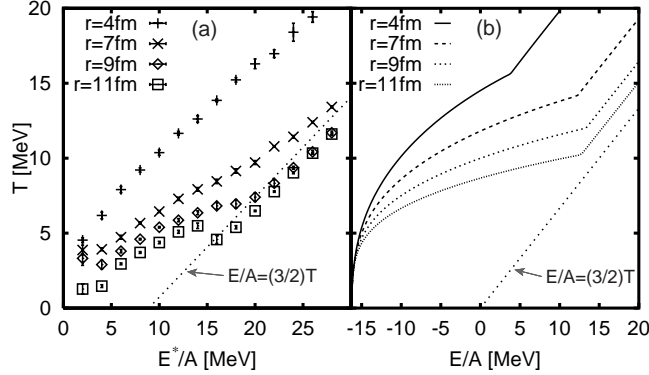


FIG. 1: (a) The constant volume caloric curves for the $A = 36$ system obtained by AMD. Statistical uncertainty is shown by error bars. The results are shown for the container size $r_{\text{wall}} = 4, 7, 9, 11$ fm. The line of $E/A = (3/2)T$ is drawn for comparison. (b) The constant volume caloric curves obtained by the Maxwell construction combined with a homogeneous Hartree-Fock calculation for the infinite nuclear matter. The curves are drawn for the average densities $36/(\frac{4}{3}\pi r_{\text{wall}}^3)$ with $r_{\text{wall}} = 4, 7, 9, 11$ fm.

obtained by applying the Maxwell construction to a homogeneous Hartree-Fock calculation with the Gogny force. The studied system with $A = 36$ shows a similar feature to the phase transition in the infinite system. The low energy part of the caloric curve corresponds to the liquid-gas phase coexistence, while the high energy part is the pure gas phase. However, plateau or backbending does not appear in the constant volume caloric curves.

It is the constant pressure caloric curve that is expected to show the signal of liquid-gas phase transition most prominently. As is well known and shown in Fig. 2b for the infinite matter, the plateau region appears in the constant pressure caloric curves when the phase transition occurs and the liquid and gas phases coexist. We show in Fig. 2a the calculated constant pressure caloric curves for the finite system with $A = 36$, which are obtained by performing the transformation between V and P by the interpolation at each energy E . The caloric curves are shown for the pressure $P = 0.02, 0.05, 0.10, 0.20, 0.30, 0.40$ MeV/fm³.

In each caloric curve with $P \lesssim 0.2$ MeV/fm³, the plateau region is observed clearly. For example at $P = 0.05$ MeV/fm³, the temperature T is almost constant below $E^*/A = 18$ MeV, while T goes up linearly with a slope $3/2$ as E^*/A increases, which implies that the system is similar to ideal gas in high energies. These features in the finite system are the same as those in the infinite matter (Fig. 2b) qualitatively. However, the boiling temperature

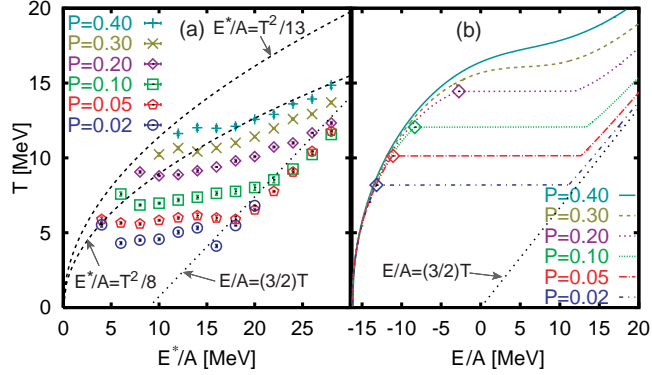


FIG. 2: (a) The constant pressure caloric curves for the $A = 36$ system obtained by AMD. Statistical uncertainty is shown by error bars. The results are shown for the pressures $P = 0.02, 0.05, 0.10, 0.20, 0.30, 0.40$ MeV/fm³. The curves of $E^*/A = T^2/(8 \text{ MeV})$, $E^*/A = T^2/(13 \text{ MeV})$ and the line of $E/A = (3/2)T$ are drawn for comparison. (b) The constant pressure caloric curves obtained by the Maxwell construction combined with a homogeneous Hartree-Fock calculation for the infinite nuclear matter.

in the finite system is significantly lower than in the infinite matter when compared at the same pressure.

In the left edge of the plateau region, the calculated result shows backbending, namely the decrease of the temperature as the energy increases, which is possible only in the first order phase transition in finite systems (more precisely, in non-extensive systems) [7, 8, 9]. This backbending effect is much larger than the statistical uncertainty in the result and is observed in all the caloric curves for $P \lesssim 0.2$ MeV/fm³. If we look at the microscopic states in the ensembles, we can see that the backbending takes place when one (or a few) large nucleus in the lowest E^*/A part breaks up suddenly into many small clusters when E^*/A is increased. In the caloric curve for a low pressure ($P = 0.02$ MeV/fm³), another kind of backbending is also observed in the high energy part of the plateau region, which occurs when small clusters (like α particles) breaks up into nucleons.

As already mentioned, the AMD calculation was not done for the pure liquid phase in Fig. 2a because of our choice of the container size $r_{\text{wall}} \geq 4$ fm. Nevertheless, we can discuss the pure liquid caloric curve in the AMD result as follows. In Fig. 2b, diamond marks are put at the points corresponding to the density for $r_{\text{wall}} = 4$ fm. The points are inside the plateau region but we can practically identify them as the left edge of the coexistence

region. Furthermore, as is seen in the infinite matter, the pure liquid caloric curves are almost independent of the pressure unless the liquid is compressed with higher pressure ($P > P_c \sim 0.4 \text{ MeV/fm}^3$). Therefore, in our AMD result in Fig. 2a, we can get the (non-compressed) liquid caloric curve by connecting the leftmost points, which can be compared to the Fermi gas formula $E^*/A = aT^2$ for excited nuclei. Our AMD result is consistent to the Fermi-Dirac statistics with a reasonable level density parameter in the range $a^{-1} = 8\text{-}13 \text{ MeV}$.

The current AMD model has an arbitrary parameter that controls how frequently the quantum branching of wave packet splittings takes place [26]. In AMD, each single-particle wave function is assumed to localize stochastically into wave packets to form clusters in individual quantum channels, which is an effect of many-body correlations (beyond the two-nucleon collision effect that is taken into account by the other branching process). The results in Figs. 1a and 2a have been obtained by taking the branching rate for each nucleon k

$$P_k = N_k/\tau_0, \quad (3)$$

where N_k is the number of other nucleons near the nucleon k in the distance of 2.5 fm. The branching rate is assumed to be proportional to N_k because the wave packet splittings are due to many-body effects and there should be no splittings for isolated nucleons. We have taken $\tau_0 = 500 \text{ fm}/c$ in the above calculations.

We should check the robustness of the obtained results against the arbitrariness of the branching rate. In Figs. 3a and 3b, the constant pressure caloric curves are shown for the cases of $\tau_0 = 250$ and $1000 \text{ fm}/c$, respectively. Moreover, Fig. 3c shows the result when we take another kind of choice of branching rate that was adopted in Ref. [26] for a nuclear collision calculation. In this case, the branching is assumed to take place for a nucleon when it is scattered by a two-nucleon collision with another nucleon. The results in Fig. 3 indicate that the plateau and backbending features are independent of the choice of the branching rate.

In the calculated results in Fig. 2, we notice that P -dependence of the AMD caloric curves in the gas phase region is different from that of the mean field values for the infinite matter. In AMD, the attractive interaction among gas nucleons is effectively weaker than in the mean field case. This is related to the treatment of light clusters such as deuterons. AMD has been constructed so that two nucleons gain only a few MeV to form a deuteron

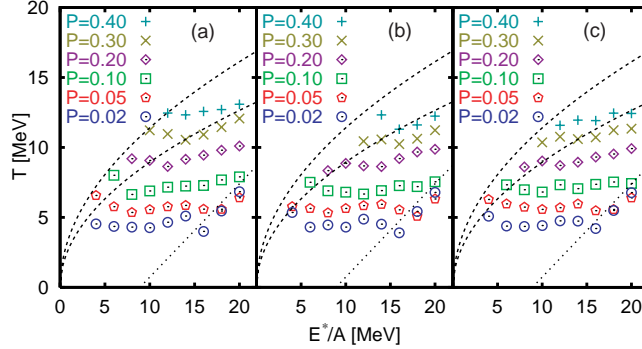


FIG. 3: The AMD results of the constant pressure caloric curves when the quantum branching rate is varied: (a) $\tau_0 = 250$ fm/c, (b) $\tau_0 = 1000$ fm/c, and (c) the same procedure as in Ref. [26].

when they approach spatially close, while much more energy should be gained in order to obtain the mean field caloric curves for gas phase. If AMD is modified so that the interaction among gas nucleons is similar to the mean field treatment, the high pressure caloric curves in Fig. 2a will shift up in the gas phase region. This will affect the critical point at which the plateau disappears. However, the backbending feature will not be affected because the low energy part of caloric curves, especially of low pressure caloric curves, should be independent of the treatment of the gas nucleon interaction because there are very few gas nucleons there.

In conclusion, we calculated the microcanonical caloric curves of a nuclear system with 36 nucleons using AMD as a model for the microscopic time evolution. We applied the same AMD model that has been used to describe nuclear reactions successfully. For the first time as a molecular dynamics calculation, we found the backbending feature in the constant pressure caloric curves. This feature is a specific character of the first order phase transition in finite systems. The obtained feature is not sensitive to the theoretical ambiguities.

[1] M. Schmidt et al., Phys. Rev. Lett. **87**, 203402 (2001), and references therein.

[2] F. Gobet et al., Phys. Rev. Lett. **87**, 203401 (2001).

[3] F. Gobet et al., Phys. Rev. Lett. **89**, 183403 (2002).

[4] D. Durand, E. Suraud, and B. Tamain, *Nuclear Dynamics In The Nucleonic Regime*, IOP-Publishing, 2000.

[5] O. Lopez, Nucl. Phys. **A685**, 246c (2001), and references therein.

- [6] S. D. Gupta, A. Z. Mekjian, and M. B. Tsang, *Adv. Nucl. Phys.* **26**, 91 (2001).
- [7] D. H. E. Gross, *Phys. Rep.* **279**, 119 (1997).
- [8] D. H. E. Gross, *Phys. Chem. Chem. Phys.* **4**, 863 (2002).
- [9] D. H. E. Gross and E. V. Votyakov, *Eur. Phys. J. B* **15**, 115 (2000).
- [10] J. Pochodzalla et al., *Phys. Rev. Lett.* **75**, 1040 (1995).
- [11] P. Chomaz and F. Gulminelli, *Nucl. Phys.* **A647**, 153 (1999).
- [12] M. D'Agostino et al., *Nucl. Phys.* **A650**, 329 (1999).
- [13] M. D'Agostino et al., *Phys. Lett. B* **473**, 219 (2000).
- [14] J. B. Natowitz et al., *Phys. Rev. C* **65**, 034618 (2002).
- [15] M. B. Tsang et al., *Phys. Rev. C* **64**, 054615 (2001).
- [16] J. B. Elliott et al., *Phys. Rev. Lett.* **88**, 042701 (2002).
- [17] J. Randrup and S. E. Koonin, *Nucl. Phys.* **A471**, 355 (1987).
- [18] J. P. Bondorf et al., *Phys. Rep* **257**, 133 (1995).
- [19] A. H. Raduta and A. R. Raduta, *Phys. Rev. Lett* **87**, 202701 (2001).
- [20] A. Ono, H. Horiuchi, T. Maruyama, and A. Ohnishi, *Phys. Rev. Lett* **68**, 2898 (1992).
- [21] A. Ono, H. Horiuchi, T. Maruyama, and A. Ohnishi, *Prog. Theor. Phys.* **87**, 1185 (1992).
- [22] J. Aichelin, *Phys. Rep.* **202**, 233 (1991).
- [23] T. Maruyama, A. Ono, A. Ohnishi, and H. Horiuchi, *Prog. Theor. Phys* **87**, 1367 (1992).
- [24] A. Ono and H. Horiuchi, *Phys. Rev. C* **53**, 2958 (1996).
- [25] A. Ono, *Phys. Rev. C* **59**, 853 (1999).
- [26] A. Ono, S. Hudan, A. Chbihi, and J. D. Frankland, *Phys. Rev. C* **66**, 014603 (2002).
- [27] H. Feldmeier, *Nucl. Phys.* **A515**, 147 (1990).
- [28] Y. Kanada-En'yo, H. Horiuchi, and A. Doté, *Phys. Rev. C* **60**, 064304 (1999), and references therein.
- [29] A. Ohnishi and J. Randrup, *Phys. Rev. Lett.* **75**, 596 (1995).
- [30] A. Ohnishi and J. Randrup, *Ann. Phys.* **253**, 279 (1997).
- [31] J. Schnack and H. Feldmeier, *Phys. Lett. B* **409**, 6 (1997).
- [32] A. Ono and H. Horiuchi, *Phys. Rev. C* **53**, 845 (1996).
- [33] A. Ono and H. Horiuchi, *Phys. Rev. C* **53**, 2341 (1996).
- [34] Y. Sugawa and H. Horiuchi, *Phys. Rev. C* **60**, 064607 (1999).
- [35] Y. Sugawa and H. Horiuchi, *Prog. Theor. Phys.* **105**, 131 (2001).

[36] J. Dechargé and D. Gogny, Phys. Rev. C **21**, 1568 (1980).

[37] A. Ono, H. Horiuchi, and T. Maruyama, Phys. Rev. C **48**, 2946 (1993).